Title: Metapopulation stability in branching river networks

Author: Akira Terui[1,2*], Nobuo Ishiyama[2], Hirokazu Urabe[3], Satoru Ono[4], Jacques C. Finlay[1], Futoshi Nakamura[2]

***Corresponding author:** E-mail: hanabi0111@gmail.com (A. Terui)

Affiliation: [1] Department of Ecology, Evolution and Behavior, University of Minnesota, 140 Gortner Laboratory, 1479 Gortner Avenue, St. Paul, MN 55108, USA; [2] Department of Forest Science, Graduate School of Agriculture, Hokkaido University, N9W9, Sapporo 060-8589, Japan; [3] Salmon and Freshwater Fisheries Research Institute, Hokkaido Research Organization, 3-373 Kitakashiwagi, Eniwa, 061-1433, Japan; [4] Institute of Environmental Sciences, Hokkaido Research Organization, N19W12, Kita-ku, Sapporo, 060-0819, Japan

Author contributions

AT conducted theoretical and statistical analyses and led manuscript writing. AT, NI, HU and SO organized the datasets. All authors participated in conception, discussion of the results and manuscript preparation.

Abstract

Intraspecific population diversity (specifically, spatial asynchrony of population dynamics) is an essential component of metapopulation stability and persistence in nature. In two-dimensional systems, theory predicts that metapopulation stability should increase with ecosystem size (or habitat network size): larger ecosystems will harbor more diverse subpopulations with more stable aggregate dynamics. However, current theories developed in simplified landscapes may be inadequate to predict emergent properties of branching ecosystems – an overlooked, but widespread habitat geometry. Here we combine theory and analyses of a unique long-term dataset to show that a scale-invariant characteristic of fractal river networks, branching complexity (measured as branching probability), stabilizes watershed metapopulations. In riverine systems, each branch (i.e., tributary) exhibits distinctive ecological dynamics, and confluences serve as “merging” points of those branches. Hence, increased levels of branching complexity should confer a greater likelihood of integrating asynchronous dynamics over the landscape. We theoretically revealed that the stabilizing effect of branching complexity is a consequence of purely probabilistic processes in natural conditions where within-branch synchrony exceeds among-branch synchrony. Contrary to current theories developed in two-dimensional systems, metapopulation size (a variable closely related to ecosystem size) had vague effects on metapopulation stability. These theoretical predictions were supported by

18-year observations of fish populations across 31 watersheds: our cross-watershed comparisons revealed consistent stabilizing effects of branching complexity on metapopulations of very different riverine fishes. A strong association between branching complexity and metapopulation stability is likely to be a pervasive feature of branching networks that strongly affects species persistence during rapid environmental changes.

Significance Statement

Metapopulation stability is a critical ecological property. Although ecosystem size has been considered as a fundamental driver of metapopulation stability, current theories developed in simplified landscapes may not be appropriate for complex branching ecosystems, such as rivers. Here, we show that a scale-independent characteristic of fractal river networks, branching complexity (measured as branching probability), stabilizes watershed metapopulations. We theoretically revealed that a strong association between branching complexity and metapopulation stability is a consequence of purely probabilistic processes. Furthermore, the stabilizing effect of branching complexity was consistently observed in metapopulations of four ecologically distinct riverine fishes. Hence, branching complexity may be a ubiquitous agent of metapopulation stability in branching ecosystems. The loss of such complexity may undermine resilience of metapopulations.

Key words: dendritic ecological network, portfolio effect, dispersal, stream, spatially structured population

/body

Introduction

Over the past few decades, there has been growing interest in understanding how the web of living organisms maintains the temporal stability of ecosystems. Much attention has been paid to diversity-stability relationships of multispecies communities (1). However, recent recognition on intraspecific population diversity – spatial and/or life-history distinctiveness among groups of individuals – has sparked discussion of how this underappreciated component of biological complexity contributes to metapopulation stability and persistence in nature (2-4). The key element of population diversity effects is the spatial asynchrony of population dynamics in metapopulations, which we define here broadly as groups of subpopulations connected via dispersal (5). Integration of multiple asynchronous dynamics over space should dampen stochastic fluctuations occurring at the level of component subpopulations, underpinning the global metapopulation stability (6, 7). Given the anticipated environmental uncertainty due to anthropogenic climate change, it is more imperative than ever to understand underlying

processes of emergent stability of metapopulations (8).

Metapopulation stability is thought to be largely determined by ecosystem size (or habitat network size; hereafter, we call it collectively as “ecosystem size”), a fundamental driver of various ecosystem properties such as food chain length (9, 10) and ecosystem production (11). Larger ecosystems will include probabilistically more diverse subpopulations, resulting in more stable metapopulation dynamics through statistical averaging (2, 12-14). In theory, this scaling relation can be expected on statistical grounds alone if all subpopulations are equally and imperfectly synchronized over the landscape, and more specifically, if synchronies for all subpopulation combinations are describable by a single correlation coefficient ρ (15). This scale-dependent nature of metapopulation stability has been commonly observed in two-dimensional systems (16-18), where the key theoretical assumption of homogeneous distributions of synchrony may hold true. In those simplified landscapes, two major forces – environmental similarity (i.e., Moran effect) and dispersal – may lead to emergence of constant synchrony at landscape scales (18-20).

A growing body of evidence suggests, however, that current theories devoted for simplified landscapes may not predict emergent properties of complex branching ecosystems – an overlooked, but widespread habitat geometry (21-26). Geomorphological or biological processes form naturally fractal branching structure (e.g., rivers, trees), in which geometric

90 statistical properties (e.g., branching complexity) remain constant across spatial scales (27-30).
91 Thus, branching structure should represent a dimension of system property that is orthogonal to
92 ecosystem size. If synchronization patterns are hierarchically organized by the branching
93 structure (i.e., a scale-invariant characteristic), then metapopulation dynamics may not be
94 describable by existing theories developed in one- or two-dimensional systems. Fluvial river
95 networks, on which humans rely for many ecosystem services (22, 31), exemplify this
96 alternative landscape (28, 32).

97 Here, we hypothesize that a scale-invariant characteristic of fractal river networks,
98 branching complexity, should stabilize the watershed metapopulation dynamics. In riverine
99 systems, an individual branch (tributary) may represent a spatial unit of synchronized ecological
100 dynamics, because subpopulations living in a same branch should experience similar
101 environmental signals (e.g., flood disturbance) (33, 34) and/or frequent mixing of individuals
102 *via* dispersal (35, 36). Meanwhile, confluences serve as "merging" points where branch-specific
103 dynamics aggregate into a larger, ecologically different downstream channel (14, 21). Therefore,
104 increased levels of branching complexity (in terms of branching prevalence) should confer a
105 greater likelihood of integrating asynchronous dynamics over the landscape.

106 In this study, using a simple theoretical model, we show that this "branching
107 complexity-stability" relationship can be a consequence of purely probabilistic processes. This

emergent phenomenon arises only if we consider systematic heterogeneity of population synchrony (i.e., differential levels of synchronization between “within-branch” and “among-branch” subpopulations), the nature of branching networks that has been overlooked in previous theoretical explorations. We further evaluated our theoretical predictions using 18-year observations of fish population abundance across 31 watersheds in Hokkaido, Japan. These small watersheds are separated by the ocean and vary greatly in branching structure due to geological and climatic differences (28). Hence, this unique long-term dataset represents ideal replication of independent river networks (see Fig. 1b and Fig. S1). We confirmed the stabilizing effect of branching complexity on metapopulations of four fish species involving three major families of freshwater fish in the northern hemisphere: *Barbatula toni* (Balitoridae), *Tribolodon hakonensis* (Cyprinidae), *Oncorhynchus masou masou*, and *Salvelinus leucomaenis* (Salmonidae). Our results demonstrate the fundamental role of branching structure in driving metapopulation stability, an important effect that underpins the long-term persistence of species in the face of increasing environmental variability.

Results

Theoretical prediction

126 We described analytical relationships between the coefficient of variation of metapopulations
127 (CV_m) and branching probability *P* (see equation 2 in Materials and Methods). Our theoretical
128 model predicted that branching complexity should dampen temporal variability of
129 metapopulations if within-branch population synchrony was greater than among-branch
130 synchrony (within-branch correlation ρ_{wb} > among-branch correlation ρ_{ab}) (lines in Fig. 2).
131 However, these relationships reversed if ρ_{ab} exceeded ρ_{wb} (Fig. 2). Metapopulation size *N* did not
132 change the relation of branching complexity and CV_m (Fig. 2).

133 Importantly, for both scenarios, stochastic simulations suggested that the uncertainty
134 of expected CV_m decreased with increasing branching probability *P* (dots in Fig. 2). This
135 stemmed from low structural variability in networks with high branching probabilities: in our
136 model, stochastic variation in the number of subpopulations within a branch (*n*) fell nonlinearly
137 as branching probability increased [$Var(n) = \frac{1-P}{P^2}$; see Materials and Methods]. This facilitated
138 greater structural stability of randomly branching networks, leading to more predictable spatial
139 synchrony and global stability patterns of metapopulations.

140 Contrary to the effects of branching complexity, effects of metapopulation size were
141 not directly related to metapopulation stability but were rather contingent upon branching
142 probability *P* (Fig. 2). As a result, vague relationships between metapopulation size and CV_m
143 were observed except when ρ_{wb} equaled ρ_{ab} (see dots in Fig. S2). Specifically, metapopulation

144 size effects were apparent only when branching probability was low ($P < 0.3$; Fig.2 and Fig. S2).
145 Therefore, the effects may be hardly detectable in real river networks, where both branching
146 probability P and metapopulation size N vary simultaneously (see dots in Fig. S2). The
147 metapopulation stability depended exclusively on N and ρ when all subpopulations were equally
148 correlated ($\rho_{wb} = \rho_{ab}$) (Fig. 2).
149 The above predictions were also supported in more realistic metapopulations. Even
150 when abundances and CVs of subpopulations were unequal (*SI Appendix*), branching
151 complexity consistently stabilized metapopulations as long as within-branch synchrony was
152 higher than among-branch synchrony (Figs. S3–8). In contrast, effects of metapopulation size
153 were unclear in most parameter settings (Figs. S9–14). Furthermore, an individual-based
154 simulation model, which incorporated detailed ecological processes that underlie population
155 synchrony (dispersal, local demography and environmental stochasticity), reproduced the
156 patterns expected from our analytical model (*SI Appendix*, Figs. S15–17). Thus, the relationship
157 of branching complexity and metapopulation stability was not sensitive to simplified theoretical
158 assumptions.
159
160 *Empirical evidence*
161 We first estimated detectability of the study species with a Bayesian multinomial model that

accounted for random variation across sites and years: thus, this approach corrects not only for imperfect detection but also for observer-specific errors (see *SI Appendix*). On average, detection probabilities were reasonably high across four study species (0.73–0.92; Table S4). The Bayesian state-space model was fitted to the detectability-corrected data. We reconstructed complete 18-year population trends of four freshwater fish species (Figs. S18–21; see also Fig. S22 for model fit check) to quantify the stability of metapopulations (CVs of watershed-scale metapopulation dynamics).

Despite the substantial variation in the ecological traits of study species (Table S3), a fixed-response model (no species-specific responses to explanatory variables; WAIC = 345.9) outperformed a variable-response model that assumed differential species responses (WAIC = 365.1). Thus, there was no statistical evidence of species-specific responses to the explanatory variables. Furthermore, the Bayesian *p*-value for the fixed response model was 0.53, indicating that the model fit was reasonably good.

In the fixed-response model, watershed metapopulation variability (CV) decreased significantly with increasing branching probability (Table 1 and Fig. 3), providing empirical evidence for the stabilizing effect of branching complexity. Moreover, as predicted by stochastic simulations, increased branching probability decreased uncertainty of watershed metapopulation stability. That is, highly fluctuating metapopulations are less likely to occur in complex river

networks (Fig. 3). Thus, branching complexity has dual important impacts on watershed metapopulation dynamics: dampening average and maximum levels of watershed metapopulation variability. Other environmental factors, including watershed area (i.e., an empirical proxy for metapopulation size *N*), had little effects on the watershed metapopulation stability (Table 1).

Discussion

Ecosystem size, a variable intimately linked to metapopulation size, has been believed to be a general predictor of metapopulation stability. However, in branching networks, size effects were poorly supported by theory (metapopulation size *N*) or empirical analyses (watershed area; an empirical proxy for metapopulation size). Instead, a scale-invariant characteristic of fractal river networks, branching complexity, emerged as an important stabilizing agent across four riverine fishes, in line with our theoretical predictions. The species-invariant effect of branching complexity implies the existence of a general statistical property underpinning watershed metapopulation stability. Our findings are particularly valuable for biodiversity conservation in complex landscapes because species living in branching ecosystems are likely to exhibit classical metapopulation dynamics that are inherently vulnerable to rapid environmental

changes (37).

Our results are in general agreement with a few previous studies suggesting that branching complexity enhances metapopulation stability or persistence (24, 25, 38, 39). However, our theoretical exploration provides two new insights into metapopulation stability under natural conditions where within-branch synchrony greatly exceeds among-branch synchrony. First, the stabilizing effect of branching complexity is an emergent phenomenon of purely probabilistic processes. Thus, our theoretical prediction should be applicable to many species inhabiting river networks and other branching ecosystems (e.g., trees, caves, mountain ranges). Second, the form of the "complexity-stability" relationships changed very little along a gradient of metapopulation size N. Hence, the impact of branching complexity should appear across a wide range of spatial scales. These two properties, which have not been recognized in previous studies, may explain why stabilizing effects of branching structure were invariant across four ecologically distinct fishes (see Table S3).

Many potential mechanisms could promote within-branch population synchrony, including external forces acting on subpopulations. A common feature of riverine systems is that environmental signals (e.g., flood disturbance) cascade down along branches of stream networks (33). Environmental conditions are highly distinctive among branches due in part to variability of local geological and geomorphological features such as slope, aspect, and soil porosity (14,

40). Such spatial patterning of environmental effects may cause subpopulation responses that are unique to each branch. Alternatively, systematic heterogeneity of population synchrony can stem from internal properties of organisms, such as dispersal. Within-branch mixing of individuals is typically more frequent than among-branch dispersal (35, 36, 41), because cross-branch movements impose longer travel distance along a network (22) or extra costs for overland dispersal [e.g., salamanders (41)] to potential dispersers. This structural constraint *per se* should enhance coherent subpopulation dynamics within a branch. In addition, the limited gene-flow across branches, combined with branch-specific environments, may foster local adaptation. Life history variation among streams (e.g., spawning timing) has been found in various aquatic organisms (40, 42, 43) and are thought to bring differential responses to shared environmental fluctuations (2). All the above mechanisms can act in concert and form the basis of the observed stabilizing effect of branching complexity.

Our theoretical model also suggested that the stabilizing effect of branching complexity should fade out, or even reverse, as among-branch population synchrony (ρ_{ab}) increases (Fig. 2). This pattern may arise from homogenization of branch-specific environmental conditions, as well as strong local demographic/environmental stochasticity. Human alterations, such as flow regulations by dams (44, 45), land use change (11, 31) and artificial propagation programs of fishes (3), have homogenized branch distinctiveness of flow,

234 physical conditions, and resource type and availability across the globe. Thus, stabilizing effects
235 of branching complexity may be diminished in severely altered landscapes. Such
236 human-induced processes could be responsible for the apparent lack of stabilizing effects of
237 branching complexity in one notable study, which assessed salmon metapopulation stability
238 across pristine and human-altered watersheds (46). In this sense, our study system offered an
239 excellent opportunity to quantify branching effects since the study watersheds had very little
240 human impact (see *SI Appendix* and Table S1). Thus, any influence of unmodeled confounding
241 factors should be minimal. Furthermore, our advanced statistical approach fostered by
242 exhaustive sampling efforts (i.e., two-pass removal across all sites for 18 years) allowed us to
243 account for unavoidable observation errors (e.g., imperfect detection), a critical issue of
244 long-term monitoring programs. These strengths may have helped to illuminate the stabilizing
245 effect of branching complexity that otherwise can be easily missed.
246 In our empirical analysis, direct comparisons between within-branch and
247 among-branch population synchronies were impossible because it requires a greater number of
248 within-network replication than available even in our large dataset. Therefore, the possibility
249 exists that other ecological processes could be responsible for our empirical results.
250 Nevertheless, we are unaware of any general theories that could provide convincing
251 explanations for the observed patterns. Furthermore, it is difficult to envision that detailed

252 ecological traits (e.g., dispersal rate), which are often species-specific, explain the consistent
253 stabilizing effect of branching complexity on very different fish species.

254 Our proposed theory arises from the physical architecture of spatial structure and is
255 applicable across a wide range of spatial scales. In addition, the wealth of indirect evidence
256 implies the existence of systematic heterogeneity of population synchrony (see above). At
257 present, our theory should best explain the observed impacts of branching complexity.

258 An intriguing avenue for future research is to ask how our findings can be scaled up to
259 metacommunities (47). Branching structure is a primary determinant of species diversity
260 patterns in experimental (48-50) and natural branching landscapes (51, 52); however, it remains
261 elusive how long-term dynamics of metacommunities are mediated by spatial network structure
262 [but see (50)]. We expect that interspecific synchrony may play an important role in determining
263 the relationship between branching complexity and metacommunity dynamics. Although the
264 present study focused on single-species metapopulations separately, an extension of our
265 framework that incorporates interspecific synchrony terms (53) may offer a promising tool to
266 predict metacommunity-level stability in branching ecosystems.

267 Branching systems are ubiquitous in nature. Biological, geomorphological, and other
268 habitat-forming processes can create fractal branching networks. In those systems, the
269 scale-invariant complexity of ecosystems can drive metapopulation stability via purely

probabilistic processes. Hence, there is no reason to believe that our fundamental finding is any less relevant for other aquatic and terrestrial organisms living in branching ecosystems. Recognition of the role of branching structure in driving metapopulation stability should increase our ability to manage and conserve species in complex landscapes.

Materials and Methods

Theory

Branching networks can be depicted by nodes connected *via* edges (25, 39, 54). In our framework, following Yeakel *et al.* (39), nodes denote populations living in discretized river sections with a scale length l, which include either non-branching or branching river sections (Fig. 1a). The scale length l defines the spatial scale of local reproductive interactions (hereafter, "subpopulation") and may depend on attributes of the species of interest such as dispersal ability. We assumed binary river networks, in which rivers bifurcate at confluences.

We define *metapopulation stability* as relative fluctuations of metapopulation abundance (or density) through time. The major goal of our theoretical exploration is to describe metapopulation stability by the following properties.

(1) **Metapopulation size N** (subpopulation $i = 1, 2, \ldots, N$). Metapopulation size

288 defines the number of interacting subpopulations and is closely related to ecosystem size L (total
289 river length of the watershed). The expected metapopulation size can be expressed as $N = L / l$.
290 For all subpopulations, we assumed equal temporal mean μ and standard deviation σ of
291 subpopulation abundance, and thus, identical coefficient of variation ($CV_p = \sigma/\mu$). Various
292 ecological processes (e.g., environmental fluctuations) impact temporal dynamics of
293 subpopulations $x(t)$. Network structure influences spatial patterning of these factors (see below).
294 (2) **Branching probability *P***. Each node is assigned to be either a branching (or
295 upstream terminal) node with probability P or a non-branching node with probability $1 - P$. In
296 this formulation, an individual branch represents a series of non-branching nodes terminated at a
297 branching (or terminal) node (equivalent to "*link*" in geomorphological term; see Fig. 1a). The
298 number of subpopulations involved in branch j (n_j) is a realization of random variable drawn
299 from a geometric distribution with success (branching) probability P [$E(n) = \frac{1}{P}; Var(n) =$
300 $\frac{1-P}{P^2}$]. In binary river networks, NP and $\frac{NP+1}{2}$ represent the expected numbers of branches and
301 source streams (1st order streams) in a network, respectively. Branching probability
302 characterizes statistical self-similarity of a theoretical river network across scales [fractal *sensu*
303 *lato*; see *SI Appendix* for details]. Note that a geometric distribution is a discrete version of an
304 exponential distribution, which has been traditionally used to describe random branch (link)
305 lengths (e.g., 55). The above procedure is equivalent to sampling a river network of

306 metapopulation size N from a pool of random river networks with branching probability P.

307 (3) **Population synchrony ρ**. We expressed the degree of population synchrony using
308 the Pearson's correlation coefficient. Specifically, we considered two levels of synchronization:
309 within-branch (ρ_{wb}) and among-branch correlations (ρ_{ab}). Any population (node) combination
310 has a correlation coefficient of either ρ_{wb} or ρ_{ab}, depending on whether the two are in the same
311 branch (see Fig. 1a). These correlation coefficients were used to characterize temporal
312 subpopulation dynamics $x(t)$. Population synchrony may emerge as a consequence of ecological
313 processes including environmental similarity and/or dispersal of individuals, among others.
314 Thus, our model includes implicitly various synchronization forces and spatial interactions.

315 The global metapopulation stability is a function of component dynamics. Temporal
316 trajectory of metapopulation abundance $X(t)$ ($X = x_1 + x_2 + \ldots + x_N$) will have a variance of:

317

318 $$Var(X) = \sum_{i=1}^{N} \sigma^2 + 2\sum_{i=1}^{N-1}\sum_{j=i+1}^{N} Cov(x_i, x_j) = N\sigma^2 + 2\{\varphi\rho_{wb}\sigma^2 + ({}_NC_2 - \varphi)\rho_{ab}\sigma^2\} \quad (1)$$

319

320 where $\varphi = \sum {}_{n_j}C_2$ for branches with $n_j \geq 2$. The parameter φ represents the total number of
321 within-branch combinations of nodes and its expected value is $E(\varphi) = \frac{N}{2}(\frac{1-P^2}{P})$ [see *SI*
322 *Appendix* for derivation]. Equation 1 shows that the temporal variance of a metapopulation is
323 dependent on the summed variances of each component subpopulation and on the summed

covariances among all possible combinations of these subpopulations. By taking the square root and dividing both sides of the equation by $N\mu$ (i.e., expected metapopulation abundance), the temporal metapopulation stability (or instability), expressed as relative fluctuations of metapopulation abundance (CV_m), can be written as:

$$CV_m = CV_p \left[\frac{1+(N-1)\rho_{ab}+(\rho_{wb}-\rho_{ab})\omega}{N}\right]^{\frac{1}{2}} \quad (2)$$

where CV_p is the CV of component subpopulations (σ/μ) and $\omega = \frac{1-P^2}{P}$. CV_p does not change the functional relationship of CV_m and *P* or *N* because equation 2 has the form of a power law. When all populations are correlated equally ($\rho_{wb} = \rho_{ab} = \rho$), equation 2 can be further reduced to:

$$CV_m = CV_p \left[\frac{1+(N-1)\rho}{N}\right]^{\frac{1}{2}} \quad (3)$$

Under this scenario, CV_m is independent of branching probability *P*. Equation 3 is identical to the equation proposed by Doak *et al.* (15), who formulated the CV for a community aggregate composed of *N* species with equivalent CVs.

We also conducted stochastic simulations to illustrate uncertainty of CV_m. We considered 3×3 combinations of parameters ($\rho_{wb} = 0.1, 0.5, 0.9$; $\rho_{ab} = 0.1, 0.5, 0.9$). This range

of correlation coefficients is comparable to values often observed in nature (e.g., 56). Under each scenario, we replicated 1000 river networks with varying branching probability P and metapopulation size N, both of which were drawn randomly from uniform distributions (range: P = 0.1–0.9; N = 50–150). Metapopulation size N was rounded before performing simulations. The number of subpopulations in branch j was sampled from a geometric distribution [$n_j \sim$ Ge(P)] until the sum of n_j equals N without truncation of any nodes in a network. CV_m was calculated using equation 1 (i.e., $CV_m = \sqrt{\mathrm{Var}(X)}/N\mu$).

Finally, we developed supplementary simulation models to confirm robustness of our theoretical predictions in realistic ecological settings. Specifically, we examined effects of the following factors: (ⅰ) unequal subpopulation abundances and CVs and (ⅱ) detailed ecological processes (e.g., dispersal) that underlie population synchrony (*SI Appendix*). All procedures were performed in R 3.2.3 (57)

Empirical test

Estimation of long-term trends of stream fish metapopulations

We assembled time series data of fish abundance across 31 protected watersheds (27 entire watersheds and 4 sub-watersheds) of Hokkaido, Japan. Long-term fish monitoring began in 1971, but effective sampling methods were introduced in 1999 (a combination of cast net

sampling and electrofishing). In each watershed, fish abundance was surveyed at 2–5 permanent sampling sites using a two-pass removal method (Fig. S1), resulting in a total of 106 sites across watersheds (mean survey area per site: 172.9 ± 115.7 m^2). Fish abundance data were collected from July to September (typically July and August) with irregular interannual intervals (0- to 3-year intervals in most cases; see Table S2 for data availability). We quantified metapopulation stability of four fish species (*B. toni*, *T. hakonensis*, *O. m. masou* and *S. leucomaenis*; see Table S3 for their ecological traits) during a period of 1999–2016. After filtering the data to remove less reliable information, the number of watersheds analyzed varied from 16 to 31 depending on species. See *SI Appendix* for further details of study locations and data selection.

In our data set, metapopulation stability was not directly comparable among the watersheds because temporal data availability varied as described above (Table S2). To overcome this difficulty, we employed a state-space modeling approach within a Bayesian framework. Bayesian state-space models can infer complete population trends from sparse time series data while accounting for observation errors (58). Therefore, this approach is one of the best options currently available for analyses of empirical population time series (16). The following Bayesian state-space model was applied to each species separately.

Data model – In our model, detectability-corrected fish abundance $N_{ti(j)}$ (year t, site j nested within watershed i; see *SI Appendix* for detectability correction) was assumed to follow a

Poisson distribution with an expected mean of $\lambda_{ti(j)}$:

$$N_{ti(j)} \sim \text{Poisson}(\lambda_{ti(j)}) \quad (4a)$$

$$\log \lambda_{ti(j)} = \log d_{\text{obs},ti(j)} + \log(AREA_{ti(j)}/100) \quad (4b)$$

where $AREA_{ti(j)}$ denotes areal sampling area (m^2) (i.e., offset term). The parameter $\log d_{\text{obs},ti(j)}$ represents the log-transformed fish density (individual 100 m^{-2}) that involves site-specific year effects (i.e., observation error). The log-transformed fish density was drawn from a normal distribution.

$$\log d_{\text{obs},ti(j)} \sim \text{Normal}(\log d_{ti(j)}, \sigma_{\text{obs}}^2) \quad (5)$$

The inclusion of parameter σ_{obs} allows us to account for random variations of site-specific year effects that may stem from ecological and/or artificial factors . For example, σ_{obs} may account for spatiotemporal variability imposed by local biotic (e.g., intraspecific competition, immigration, etc.) and abiotic processes. Thus, the mean parameter $\log d_{ti(j)}$ represents "unbiased" fish density at the site scale (hereafter, "local density").

Process model – The local density $\log d_{ti(j)}$ was then described as deviation from the

396 temporal metapopulation trajectory:

397

398 $\log d_{ti(j)} = \log D_{ti} + \alpha_{i(j)}$ (5a)

399 $\alpha_{i(j)} \sim \text{Normal}(0, \sigma_{\alpha}^{2})$ (5b)

400

401 where the parameter σ_{α} governs the degree of deviation from the metapopulation-level density in
402 year *t* and watershed *i* ($\log D_{ti}$). This model assumption is robust and conservative, as no single
403 "litmus test" exists to determine whether the local aggregations are independent subpopulations
404 or parts of a larger panmictic population in a stream continuum (59, 60).

405 The temporal trajectory of metapopulation-level density $\log D_{ti}$, i.e., an empirical
406 proxy for theoretical metapopulation trajectory *X*(t), was modeled as follows:

407

408 $\log D_{[t+1]i} = \log r_{ti} + \log D_{ti}$ (6)

409

410 where $\log r_{ti}$ is the log-transformed metapopulation growth rate in year *t* and watershed *i*. We
411 assumed density-independent metapopulation growth rates because intraspecific competition is
412 unlikely to operate at a watershed scale. This is a common implicit assumption made in previous
413 empirical and theoretical studies (2, 8, 61). The log-transformed metapopulation growth was

assumed to follow a multivariate normal distribution:

$$\log r_{ti} \sim \mathrm{MN}(\boldsymbol{\zeta}, \Sigma_r) \quad (7)$$

where $\boldsymbol{\zeta}$ is the vector of watershed-specific temporal mean of metapopulation growth rate (i.e., $\log r_{\mathrm{mean},1}$, $\log r_{\mathrm{mean},2}$, …) and Σ_r represents the variance-covariance matrix of $\log r_{ti}$. The advantage of this hierarchical structure is that parameter estimates of each watershed can be improved over those that would be obtained by fitting separate watershed-specific models (62). This is apparent in our data set, because data-poor watersheds can borrow information from data-rich watersheds.

Vague priors were assigned to the parameters: i.e., normal distributions for $\log r_{\mathrm{mean}}$ (mean = 0, variance = 10^3), an inverse-Wishart distribution for Σ_r (*d.f.* = n+1, where n is the number of watersheds analyzed), and truncated normal distributions for σ_{obs} and σ_α (mean = 0, variance = 10^3, range = 0–30). The model was fitted to the data using JAGS (ver. 4.1.0) and the package "*runjags*" (63) in R 3.2.3 (57). Three Markov Chain Monte Carlo (MCMC) chains were run with 75,000 iterations (25,000 burn-in), and 500 samples per chain were used to calculate posterior probabilities. Convergence was assessed by examining whether the R-hat indicator of each parameter approached a value of one (64).

Using median estimates, we quantified the metapopulation stability. Specifically, we calculated CVs of watershed metapopulation trajectory D_{ti}. Detrending was performed before the calculation to avoid biased estimates of CVs (61): SD of residuals from a fitted lowess smoother (function "*lowess*"; a smoothing span of 2/3 of the data) was divided by the original (i.e., before detrending) temporal mean of D_{ti}.

Watershed characteristics

We estimated watershed characteristics (branching probability, watershed area) and climatic variables (annual cumulative precipitation, mean air temperature) using QGIS ver 2.12.3 (available at http://qgis.osgeo.org). Branching probability was estimated by fitting exponential distributions to histograms of branch length (km; river segment between successive confluences or a confluence and the outlet/upstream terminal) for each watershed as *Branch length* ~ Exp(υ) (55). An exponential distribution is a continuous version of a geometric distribution, and a derived statistical quantity $1 - e^{-\upsilon}$ corresponds to the theoretical branching probability P. We used river polylines (defined as >1 km^2 watershed area) of the entire watershed for the estimation of branching probability. Watershed area was used as a proxy for metapopulation size and calculated as the entire drainage area upstream of the ocean outlet (27 watersheds) or confluence with another major tributary (4 sub-watersheds; if all sampling sites were located in

450 a sub-watershed). All watershed characteristics were calculated based on the digital elevation
451 map of 90-m resolution (available at https://lta.cr.usgs.gov). Climatic variables were obtained
452 from Japan Meteorological Agency (available at http://nlftp.mlit.go.jp/ksj/index.html). We used
453 10-km mesh data of annual cumulative precipitation and mean air temperature (averaged for
454 1981–2010). We averaged values of climate meshes for each watershed. Finally, to examine the
455 influence of fish stocking on metapopulation stability, we obtained a record of cumulative
456 number of hatchery fish (masu salmon *O. m. masou*) released into each watershed during a
457 period of 1955–2016.
458 Elevation, watershed land cover and weir density were not used in the following
459 regression analysis because these variables were less informative and/or risked influences of
460 multicollinearity. See *SI Appendix* for detailed variable selection procedure.
461
462 *Stability analysis*
463 We fitted hierarchical log-normal models to estimated CVs using JAGS (ver. 4.1.0) to
464 investigate impacts of watershed characteristics on metapopulation stability. Log-transformed
465 CVs met the normality assumption (Shapiro-Wilk normality test for residuals; $p > 0.58$) and had
466 no statistically-evident outliers (Grubbs' test; $p = 0.42$). The detrended $CV_{s(i)}$ (watershed i for
467 species s) was modeled as:

468

469 $\log CV_{s(i)} \sim \text{Normal}(\mu_{s(i)}, \sigma_{cv}^2)$

470 $\mu_{s(i)} = \beta_{0,s} + \beta_{1,s} \times BP_i + \beta_{2,s} \times \log WA_i + \beta_{3,s} \times Prep_i + \beta_{4,s} \times Temp_i + \beta_5 \times Hatchery_i + \beta_6 \times Nsite_i$

471

472 where BP_i, WA_i, $Prep_i$, $Temp_i$ and $Hatchery_i$ denote branching probability, watershed area (km^2),

473 cumulative precipitation (mm), air temperature (℃), and the cumulative number of hatchery fish

474 released, respectively. $Nsite_i$ is the number of sampling sites in watershed *i* and was included as

475 a control variable. Since $Hatchery_i$ was positively correlated with WA_i (Pearson's $r = 0.72$), we

476 used residuals of a linear relationship fitted between $Hatchery_i$ and WA_i to avoid

477 multicollinearity. The residuals provide a relative measure of $Hatchery_i$, independent of WA_i

478 (e.g., positive residuals indicate greater than expected values from a linear regression). All

479 explanatory variables were standardized before the analysis (mean = 0, SD = 1).

480 We constructed two competing models: fixed-response (random intercept) and

481 variable-response models (random intercept and slope). In a fixed-response model, only does

482 the intercept $\beta_{0,s}$ vary randomly by species [$\beta_{0,s} \sim \text{Normal}(\beta_{0,global}, \sigma_{\beta 0}^2)$] while keeping slopes

483 constant among species ($\beta_{k,constant} = \beta_{k,s}$ for k = 1–6]. On the other hand, in a variable-response

484 model, both the intercept and slopes vary randomly among species [$\beta_{k,s} \sim \text{Normal}(\beta_{k,global}, \sigma_{\beta k}^2)$

485 for k = 0–6]. To compare the two competing models, we calculated the Widely Applicable

Information Criterion (WAIC) (65) using the R package "*loo*". The WAIC provides, like other information criteria, a measure of model fit that is penalized by model complexity, but has a sound theoretical foundation in Bayesian statistics and an applicability to complex hierarchical models like ours. We also checked the model performance with a Bayesian *p*-value. The Bayesian *p*-value, which was based on a sums-of-square discrepancy, approaches 0.5 if the model perfectly reproduces the data (66).

Vague priors were assigned to the parameters, i.e., normal distributions for $\beta_{k,constant}$ and $\beta_{k,global}$ (mean = 0, variance = 10^4) and truncated normal distributions for σ_{cv} and $\sigma_{\beta k}$ (mean = 0, variance = 10^4, range = 0–100). Three MCMC chains were run with 7500 iterations (2500 burn-in), and 500 samples per chain were used to calculate posterior probabilities. Convergence was assessed as described above.

Data accessibility

The codes (R and JAGS) and data reported in this study are available at *SI Appendix*.

Acknowledgements

We thank the numerous people who worked hard to collect and organize the large data sets of protected watersheds. We are grateful to Shota Nishijima, Keisuke Atsumi and Shin-ichiro S.

Matsuzaki for their constructive comments on the early draft. We thank Jesús N. Pinto-Ledezma, Josep Padullés Cubino and theory group in University of Minnesota for helpful discussion. This research was partly supported by JSPS KAKENHI to AT (no. 18K06404).

References

1. Tilman D, Isbell F, & Cowles JM (2014) Biodiversity and Ecosystem Functioning. *Annual Review of Ecology, Evolution, and Systematics* 45:471-493.
2. Schindler DE, *et al.* (2010) Population diversity and the portfolio effect in an exploited species. *Nature* 465:609-612.
3. Moore JW, McClure M, Rogers LA, & Schindler DE (2010) Synchronization and portfolio performance of threatened salmon. *Conservation Letters* 3:340-348.
4. Schindler DE, Armstrong JB, & Reed TE (2015) The portfolio concept in ecology and evolution. *Frontiers in Ecology and the Environment* 13:257-263.
5. Hanski I & Gilpin M (1991) Metapopulation dynamics: brief history and conceptual domain. *Biological Journal of the Linnean Society* 42:3-16.
6. Heino M, Kaitala V, Ranta E, & Lindström J (1997) Synchronous dynamics and rates of extinction in spatially structured populations. *Proceedings of the Royal Society of London B: Biological Sciences* 264:481-486.
7. Dey S & Joshi A (2006) Stability via asynchrony in Drosophila metapopulations with low migration rates. *Science* 312:434-436.
8. Anderson SC, Moore JW, McClure MM, Dulvy NK, & Cooper AB (2015) Portfolio conservation of metapopulations under climate change. *Ecological Applications* 25:559-572.
9. Sabo JL, Finlay JC, Kennedy T, & Post DM (2010) The role of discharge variation in scaling of drainage area and food chain length in rivers. *Science* 330:965-967.
10. Takimoto G, Spiller DA, & Post DM (2008) Ecosystem size, but not disturbance, determines food-chain length on islands of the Bahamas. *Ecology* 89:3001-3007.
11. Finlay JC (2011) Stream size and human influences on ecosystem production in river networks. *Ecosphere* 2:art87.
12. Levin SA (1992) The problem of pattern and scale in ecology: the Robert H. MacArthur award lecture. *Ecology* 73:1943-1967.
13. Wang S, Haegeman B, & Loreau M (2015) Dispersal and metapopulation stability. *PeerJ* 3:e1295.
14. Moore JW, *et al.* (2015) Emergent stability in a large, free‐flowing watershed. *Ecology*

96:340-347.

15. Doak DF, *et al.* (1998) The statistical inevitability of stability‐diversity relationships in community ecology. *The American Naturalist* 151:264-276.

16. Matsuzaki SS & Kadoya T (2015) Trends and stability of inland fishery resources in Japanese lakes: introduction of exotic piscivores as a driver. *Ecological Applications* 25:1420-1432.

17. Shelton AO, *et al.* (2017) Forty years of seagrass population stability and resilience in an urbanizing estuary. *Journal of Ecology* 105:458-470.

18. Sutcliffe OL, Thomas CD, & Moss D (1996) Spatial synchrony and asynchrony in butterfly population dynamics. *Journal of Animal Ecology* 65:85-95.

19. Hanski I & Woiwod IP (1993) Spatial synchrony in the dynamics of moth and aphid populations. *Journal of Animal Ecology* 62:656-668.

20. Pomara LY & Zuckerberg B (2017) Climate variability drives population cycling and synchrony. *Diversity and Distributions* 23:421-434.

21. Grant EHC, Lowe WH, & Fagan WF (2007) Living in the branches: population dynamics and ecological processes in dendritic networks. *Ecology Letters* 10:165-175.

22. Altermatt F (2013) Diversity in riverine metacommunities: a network perspective. *Aquatic Ecology* 47:365-377.

23. Mari L, Casagrandi R, Bertuzzo E, Rinaldo A, & Gatto M (2014) Metapopulation persistence and species spread in river networks. *Ecology Letters*.

24. Grant EHC (2011) Structural complexity, movement bias, and metapopulation extinction risk in dendritic ecological networks. *Journal of the North American Benthological Society* 30:252-258.

25. Fagan WF (2002) Connectivity, fragmentation, and extinction risk in dendritic metapopulations. *Ecology* 83:3243-3249.

26. Tonkin JD, *et al.* (2018) The role of dispersal in river network metacommunities: Patterns, processes, and pathways. *Freshwater Biology* 63:141-163.

27. Rinaldo A, Rigon R, Banavar JR, Maritan A, & Rodriguez-Iturbe I (2014) Evolution and selection of river networks: Statics, dynamics, and complexity. *Proceedings of the National Academy of Sciences* 111:2417-2424.

28. Rodríguez-Iturbe I & Rinaldo A (2001) *Fractal river basins: chance and self-organization* (Cambridge University Press, New York, NY).

29. Mandelbrot BB & Pignoni R (1983) *The fractal geometry of nature* (Freeman, New York, NY).

30. Veitzer SA & Gupta VK (2000) Random self‐similar river networks and derivations of generalized Horton laws in terms of statistical simple scaling. *Water Resources Research* 36:1033-1048.

31. Allan JD & Castillo MM (2007) *Stream ecology: structure and function of running waters* (Springer Science & Business Media, Dordrecht, Netherland).

32. Rinaldo A, Gatto M, & Rodriguez-Iturbe I (2018) River networks as ecological corridors: A coherent ecohydrological perspective. *Advances in Water Resources* 112:27-58.
33. Nakamura F, Swanson FJ, & Wondzell SM (2000) Disturbance regimes of stream and riparian systems-a disturbance-cascade perspective. *Hydrological Processes* 14:2849-2860.
34. Benda L, *et al.* (2004) The network dynamics hypothesis: how channel networks structure riverine habitats. *Bioscience* 54:413-427.
35. Macneale KH, Peckarsky BL, & Likens GE (2005) Stable isotopes identify dispersal patterns of stonefly populations living along stream corridors. *Freshwater Biology* 50:1117-1130.
36. Junker J, *et al.* (2012) River fragmentation increases localized population genetic structure and enhances asymmetry of dispersal in bullhead (*Cottus gobio*). *Conservation Genetics* 13:545-556.
37. Fronhofer EA & Altermatt F (2017) Classical metapopulation dynamics and eco-evolutionary feedbacks in dendritic networks. *Ecography* 40:1455-1466.
38. Terui A, *et al.* (2014) Asymmetric dispersal structures a riverine metapopulation of the freshwater pearl mussel *Margaritifera laevis. Ecology and Evolution* 4:3004-3014.
39. Yeakel JD, Moore JW, Guimaraes PR, & de Aguiar MAM (2014) Synchronisation and stability in river metapopulation networks. *Ecology Letters* 17:273-283.
40. Lisi PJ, Schindler DE, Bentley KT, & Pess GR (2013) Association between geomorphic attributes of watersheds, water temperature, and salmon spawn timing in Alaskan streams. *Geomorphology* 185:78-86.
41. Grant EHC, Nichols JD, Lowe WH, & Fagan WF (2010) Use of multiple dispersal pathways facilitates amphibian persistence in stream networks. *Proceedings of the National Academy of Sciences* 107:6936-6940.
42. Moore JW & Schindler DE (2010) Spawning salmon and the phenology of emergence in stream insects. *Proceedings of the Royal Society B: Biological Sciences* 277:1695-1703.
43. Lytle DA & Poff NL (2004) Adaptation to natural flow regimes. *Trends in Ecology & Evolution* 19:94-100.
44. Poff NL, Olden JD, Merritt DM, & Pepin DM (2007) Homogenization of regional river dynamics by dams and global biodiversity implications. *Proceedings of the National Academy of Sciences* 104:5732-5737.
45. Poff NL, *et al.* (1997) The natural flow regime. *Bioscience* 47:769-784.
46. Griffiths JR, *et al.* (2014) Performance of salmon fishery portfolios across western North America. *Journal of Applied Ecology* 51:1554-1563.
47. Leibold MA, *et al.* (2004) The metacommunity concept: a framework for multi-scale community ecology. *Ecology Letters* 7:601-613.
48. Carrara F, Altermatt F, Rodriguez-Iturbe I, & Rinaldo A (2012) Dendritic connectivity controls biodiversity patterns in experimental metacommunities. *Proceedings of the National Academy of*

Sciences 109:5761-5766.

49. Carrara F, Rinaldo A, Giometto A, & Altermatt F (2014) Complex interaction of dendritic connectivity and hierarchical patch size on biodiversity in river-like landscapes. *American Naturalist* 183:13-25.

50. Seymour M, Fronhofer EA, & Altermatt F (2015) Dendritic network structure and dispersal affect temporal dynamics of diversity and species persistence. *Oikos* 124:908-916.

51. Brown BL & Swan CM (2010) Dendritic network structure constrains metacommunity properties in riverine ecosystems. *Journal of Animal Ecology* 79:571-580.

52. Tonkin JD, *et al.* (2017) Metacommunity structuring in Himalayan streams over large elevational gradients: the role of dispersal routes and niche characteristics. *Journal of Biogeography* 44:62-74.

53. Delsol R, Loreau M, & Haegeman B (2018) The relationship between the spatial scaling of biodiversity and ecosystem stability. *Global Ecology and Biogeography*.

54. Eros T, Schmera D, & Schick RS (2011) Network thinking in riverscape conservation - a graph-based approach. *Biological Conservation* 144:184-192.

55. Peckham SD & Gupta VK (1999) A reformulation of Horton's laws for large river networks in terms of statistical self‐similarity. *Water Resources Research* 35:2763-2777.

56. Rogers LA & Schindler DE (2008) Asynchrony in population dynamics of sockeye salmon in southwest Alaska. *Oikos* 117:1578-1586.

57. RCoreTeam (2016) R: A language and environment for statistical computing. R Foundation for Statistical Computing, Vienna, Austria. https://www.R-project.org/.

58. Kéry M & Schaub M (2012) *Bayesian population analysis using WinBUGS: a hierarchical perspective* (Academic Press, Waltham, MA).

59. Quinn TP, Rich HB, Gosse D, & Schtickzelle N (2012) Population dynamics and asynchrony at fine spatial scales: a case history of sockeye salmon (*Oncorhynchus nerka*) population structure in Alaska, USA. *Canadian Journal of Fisheries and Aquatic Sciences* 69:297-306.

60. Schtickzelle N & Quinn TP (2007) A metapopulation perspective for salmon and other anadromous fish. *Fish and Fisheries* 8:297-314.

61. Anderson SC, Cooper AB, & Dulvy NK (2013) Ecological prophets: quantifying metapopulation portfolio effects. *Methods in Ecology and Evolution* 4:971-981.

62. Lunn D, Jackson C, Best N, Thomas A, & Spiegelhalter D (2012) *The BUGS book: A practical introduction to Bayesian analysis* (CRC press, Boca Raton, FL).

63. Denwood MJ (2016) runjags: An R package providing interface utilities, model templates, parallel computing methods and additional distributions for MCMC models in JAGS. *Journal of Statistical Software* 71:1-25.

64. Gelman A & Hill J (2007) *Data Analysis Using Regression and Multilevel/Hierarchical Models*

(Cambridge University Press, New York, NY).

65. Watanabe S (2010) Asymptotic equivalence of Bayes cross validation and widely applicable information criterion in singular learning theory. *Journal of Machine Learning Research* 11:3571-3594.

66. Kéry M (2010) *Introduction to WinBUGS for Ecologists: A Bayesian Approach to Regression, ANOVA, Mixed Models and Related Analyses.* (Academic Press, Burlington, MA).

Figure captions

Figure 1 (a) Framework for developing random river networks as a function of scale length l (i.e., spatial scale of subpopulation), metapopulation size N and branching probability P. Metapopulation size N defines the number of interacting subpopulations (the number of nodes in the lower panel) in a network. Each node with scale length l is assigned to be either a branching (or upstream terminal) node with probability P or a non-branching node with probability $1 - P$. Filled nodes in the bottom panel represent branching (or terminal) river sections while open nodes denote non-branching river sections. The arrows "*wb*" and "*ab*" denote examples of "within-branch" and "among-branch" combinations of nodes, respectively. Nodes grouped in shade represent an individual branch. (b) Map of Hokkaido island, Japan. Shaded areas are the 31 independent watersheds (separated by the ocean) where fish monitoring programs have been carried out. (c) Example from one watershed (Nikanbetsu watershed) with gray dots denoting sampling sites of fish abundance surveys.

Figure 2 Theoretical predictions for relationships of branching complexity and metapopulation stability. Different panels denote differential combinations of within-branch (ρ_{wb}) and among-branch population synchronies (ρ_{ab}) [$\rho_{wb} = \rho_{ab}$ (a, e, i); $\rho_{wb} > \rho_{ab}$ (d, g, h); $\rho_{wb} < \rho_{ab}$ (b, c, f)]. Lower CVs indicate greater temporal stability of metapopulations in branching networks. Lines are analytical predictions of metapopulation stability and different line types denote predictions with differential metapopulation sizes (solid, N = 50; broken, 100; broken-dot, 150). Dots are the results of stochastic simulations and are colored in proportion to metapopulation size N (range: 50–150; from red to ivory). CV_p was set to be 1 for simplicity (see equation 2).

Figure 3 Empirical evidence for the stabilizing effect of branching complexity (probability of branching) on stream fish metapopulations. Lower CVs indicate greater temporal stability of metapopulations. The solid line represents values predicted by the fixed-response model (median; Table 1). Shades are proportional to the posterior density. Points are stability of fish metapopulations observed across 31 watersheds for 18 years (square, *Barbatula toni;* diamond, *Tribolodon hakonensis*; triangle, *Oncorhynchus masou masou*; circle, *Salvelinus leucomaenis*).

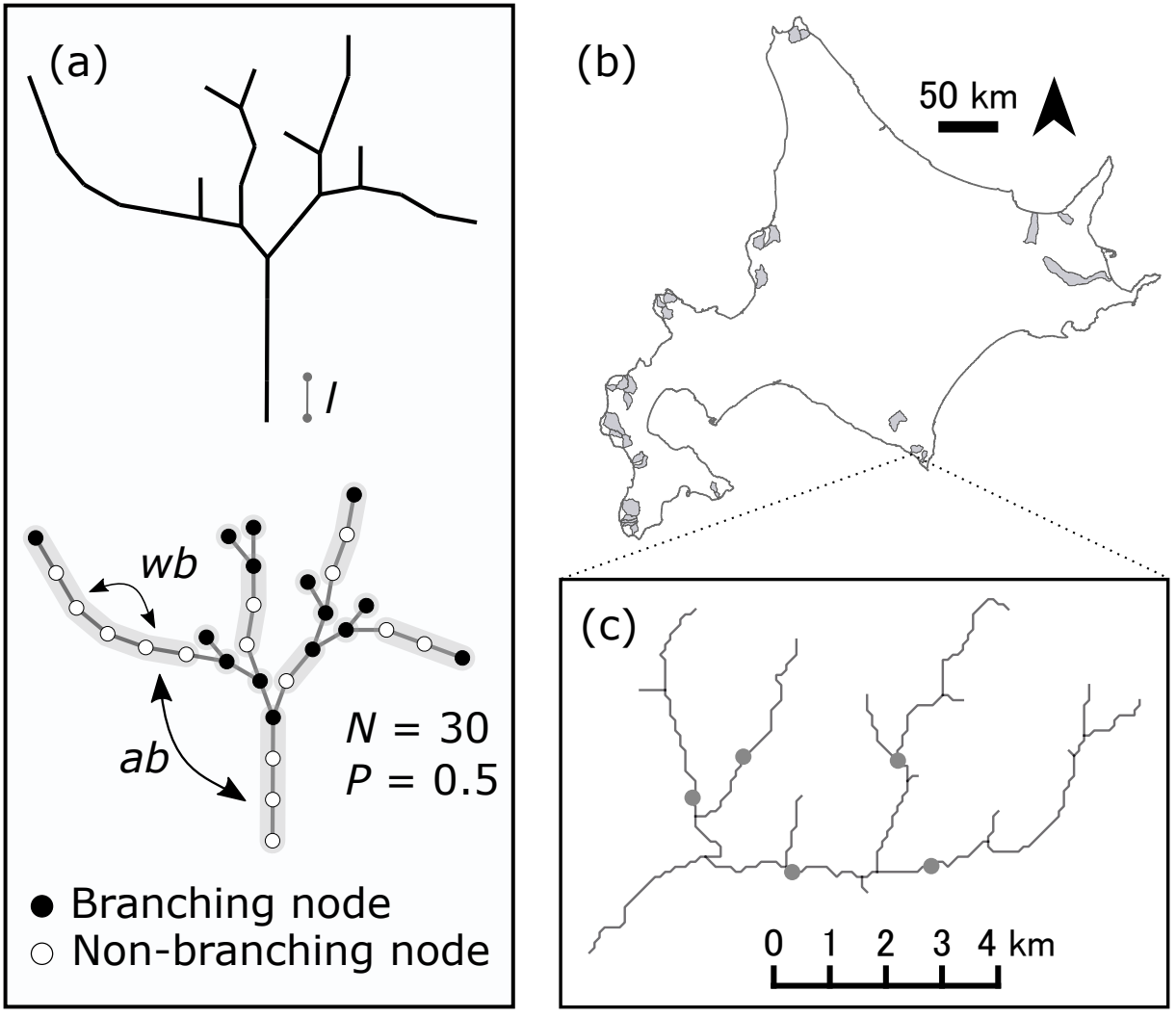
(a)
l
wb
ab
N = 30
P = 0.5
Branching node
Non-branching node
(b)
50 km
(c)
0 1 2 3 4 km

(a) (ρ_{wb},ρ_{ab}) = (0.1,0.1)

(b) (ρ_{wb},ρ_{ab}) = (0.1,0.5)

(c) (ρ_{wb},ρ_{ab}) = (0.1,0.9)

(d) (ρ_{wb},ρ_{ab}) = (0.5,0.1)

(e) (ρ_{wb},ρ_{ab}) = (0.5,0.5)

(f) (ρ_{wb},ρ_{ab}) = (0.5,0.9)

(g) (ρ_{wb},ρ_{ab}) = (0.9,0.1)

(h) (ρ_{wb},ρ_{ab}) = (0.9,0.5)

(i) (ρ_{wb},ρ_{ab}) = (0.9,0.9)

CV

Branching probability

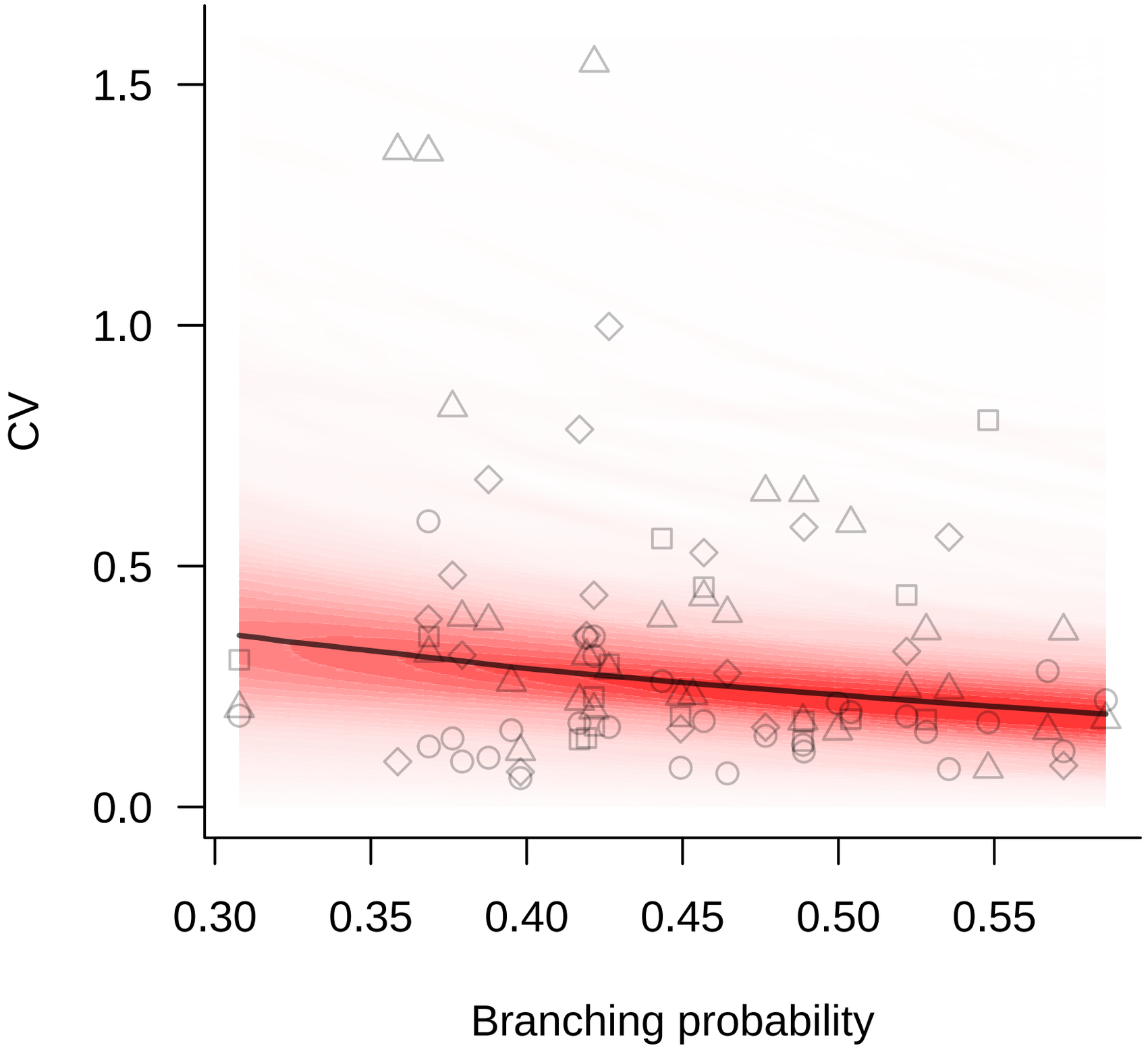
1.5
1.0
0.5
0.0
CV
0.30
0.35
0.40
0.45
0.50
0.55
Branching probability

Table 1 Results of the Bayesian hierarchical model explaining metapopulation stability of four riverine fishes (CV). Variables whose 95% credible intervals (95% CI) did not include zero were shown in bold.

Parameter	Effect	Median	95% CI
$\beta_{0,\ global}$	Intercept	**−1.36**	**−2.30 to −0.43**
β_1	Branching probability	**−0.15**	**−0.30 to −0.01**
β_2	Watershed area	0.01	−0.15 to 0.16
β_3	Temperature	−0.15	−0.30 to 0.02
β_4	Precipitation	0.14	−0.03 to 0.30
β_5	Hatchery fish	0.01	−0.13 to 0.16
β_6	Number of sampling sites	0.00	−0.16 to 0.16